

# Automated Generation of Continuous-Space Roadmaps for Routing Mobile Robot Fleets

Marvin Rüdert

Dept. Material Handling and Logistics  
Karlsruhe Institute of Technology  
Karlsruhe, Germany  
0009-0003-9853-4974

Constantin Enke

Dept. Material Handling and Logistics  
Karlsruhe Institute of Technology  
Karlsruhe, Germany  
0000-0002-4159-6862

Kai Furmans

Dept. Material Handling and Logistics  
Karlsruhe Institute of Technology  
Karlsruhe, Germany  
0000-0001-6009-5564

**Abstract**—Efficient routing of mobile robot fleets is crucial in intralogistics, where delays and deadlocks can substantially reduce system throughput. Roadmap design, specifying feasible transport routes, directly affects fleet coordination and computational performance. Existing approaches are either grid-based, compromising geometric precision, or continuous-space approaches that disregard practical constraints. This paper presents an automated roadmap generation approach that bridges this gap by operating in continuous-space, integrating station-to-station transport demand and enforcing minimum distance constraints for nodes and edges. By combining free space discretization, transport demand-driven  $K$ -shortest-path optimization, and path smoothing, the approach produces roadmaps tailored to intralogistics applications. Evaluation across multiple intralogistics use cases demonstrates that the proposed approach consistently outperforms established baselines (4-connected grid, 8-connected grid, and random sampling), achieving lower structural complexity, higher redundancy, and near-optimal path lengths, enabling efficient and robust routing of mobile robot fleets.

**Index Terms**—roadmap generation, continuous-space roadmap, mobile robot fleet, multi robot, logistics automation

## I. INTRODUCTION

The growing complexity and dynamics of modern intralogistics have intensified interest in mobile robot systems for material transport [1]. Such systems can enhance transport efficiency, reduce operational costs, and adapt flexibly to layout changes and fluctuating transport demand [2]. Achieving high system throughput and efficient fleet coordination depends not only on the fleet management system but also fundamentally on the design of the underlying roadmap [1]. A roadmap is a graph-based representation of the free space, where nodes denote discrete physical positions and edges represent feasible connections. In this work, edges are assumed to be straight, and the term *mobile robot* encompasses both Automated Guided Vehicles (AGVs) and Autonomous Mobile Robots (AMRs), which are capable of following such virtual roadmaps.

Roadmap design for mobile robot fleets involves a fundamental trade-off between redundancy and complexity. Redundancy, defined as the availability of alternative paths, enables robust coordination and reduces the risk of delays and deadlocks. In contrast, complexity, determined by the number

of nodes and edges, affects the query efficiency of routing algorithms and can cause severe performance degradation in large-scale systems [3]. Beyond this trade-off, routing efficiency, evaluated by the travel distance of the robots between stations, is a decisive factor for system throughput. Practical designs also impose minimum distance constraints for nodes and edges to ensure an efficient utilization of the roadmap.

Despite their importance, roadmaps in industrial practice are still predominantly generated manually by domain experts due to the complexity and variability of real-world systems [4]. This manual process is time-consuming, costly and often leads to suboptimal solutions [2], [5]. As a result, frequent adaptation of roadmaps to dynamic changes in layout or transport demand remains largely impractical, limiting system flexibility. Therefore, automated roadmap generation is essential to exploit the full potential of mobile robot fleets, enabling fast, data-driven adjustments while minimizing human intervention.

Automated roadmap generation has been explored from several perspectives. Classical single-robot path planning algorithms, such as the probabilistic roadmap method (PRM) [6], visibility graphs [7], rapidly-exploring random trees (RRT) [8], and Voronoi diagrams [9] are foundational for navigating known environments. While seminal, these methods were not designed for routing mobile robot fleets, lacking mechanisms to ensure sufficient redundancy for an entire fleet [5].

To address the specific requirements of mobile robot fleets, one major line of research has focused on grid-based discretization. These methods typically divide the free space into a 4-connected grid. On this basis, various methods have been developed using reinforcement learning [10], ant colony optimization (ACO) [1], [4], [11], shortest path algorithms combined with fuzzy logic to incorporate expert knowledge [12], [13], or rule-based algorithms [14].

Most of these approaches reduce roadmap complexity by pruning grid nodes that are irrelevant to the specified transport demand and by defining constraints on the grid connections. However, some methods, such as [14], focus solely on assigning connection constraints without performing node pruning. In [10] a whole intralogistics problem, defined by the layout of the environment, task distribution, fleet size and dispatching algorithm, is used as input to the roadmap generation method.

This allows to adaptively adjust the required level of redundancy based on the problem configuration.

While grid-based approaches stand out by their conceptual simplicity and are well-suited for large robot fleets, they are fundamentally constrained by their spatial resolution. This limitation prevents high-fidelity modeling of real-world environments, restricting precise placement of objects. Furthermore, it limits the achievable path lengths between stations in the layout to the Manhattan distance, which may significantly deviate from the shortest paths in continuous-space.

A second major line of research focuses on continuous-space roadmaps, which provide greater geometric accuracy and flexibility. These approaches operate in continuous-space, using a variety of techniques to discretize the free space. Examples include the medial axis transform followed by linear programming optimization [15] or rule-based algorithms [5], [16], [17], random sampling combined with stochastic gradient descent (SGD) optimization and Delaunay triangulation [18], Gray-Scott reaction-diffusion system combined with Delaunay triangulation [3], and iterative Voronoi diagram generation incorporating imaginary obstacles [19].

These methods generally aim to distribute nodes uniformly across the free space and generate well-connected roadmaps. In [5], a rule-based roadmap generation strategy is presented that explicitly accounts for robot dimensions and available space within corridors and intersections. Their goal is to maximize coverage, connectivity, and redundancy to enhance routing flexibility and system throughput. The method is evaluated using graph-theoretical metrics and is extended in [16] to support more cluttered environments. A broader evaluation framework based on graph theory is introduced in [17].

The main advantage of continuous-space approaches is their ability to produce tailored roadmaps that are not constrained by spacial resolution. However, practical distance constraints for nodes and edges are often neglected, such as in [18] and [3]. Additionally, none of the continuous-space approaches considers stations and a specified transport demand. Instead, they only aim to generate well-connected roadmaps with high coverage of the free space.

The existing literature reveals a critical gap: grid-based methods are well-suited for large mobile robot fleets but geometrically constrained, while continuous-space methods are geometrically flexible but often lack practical distance constraints required for efficient roadmap utilization. This paper introduces a novel approach that bridges this gap by automating the generation of continuous-space roadmaps tailored specifically for efficient mobile robot fleet coordination.

The main contributions of this paper are:

- 1) A transport demand-driven approach that generates continuous-space roadmaps with short, redundant paths between stations while limiting roadmap complexity.
- 2) Explicit integration of minimum distance constraints for nodes and edges, ensuring an efficient roadmap utilization with minimal blocking by the mobile robots.
- 3) A high-fidelity modeling approach operating directly in continuous-space, enabling the generation of tailored

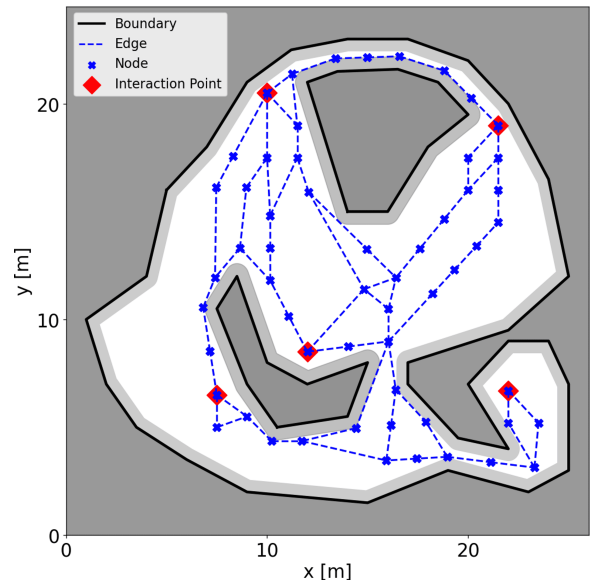


Fig. 1. Roadmap of an abstract environment. Station interaction points are connected by a roadmap consisting of nodes and edges. The roadmap adapts to environmental boundaries around obstacles (gray areas), which are geometrically expanded (light gray areas), while providing redundant, continuous-space paths within free space (white areas).

roadmaps with high geometric flexibility.

Fig. 1 illustrates a roadmap generated by the proposed approach for an abstract environment, demonstrating its ability to generate efficient roadmaps adapted to specific environmental and operational constraints.

The remainder of this paper is organized as follows. Section II defines the problem and key assumptions. Section III presents the proposed roadmap generation approach. Section IV and Section V describe the evaluation methodology and discuss the experimental results. Finally, Section VI concludes the paper and outlines future work.

## II. PROBLEM FORMULATION

The objective of the proposed approach is to automatically generate continuous-space roadmaps that enable high system throughput for mobile robot fleets. Specifically, it addresses the trade-off between providing redundant roadmaps with high routing efficiency to minimize robot travel distances and reduce their waiting times, and limiting roadmap complexity based on the transport demand to ensure query efficiency.

The proposed roadmap generation approach combines a digital map of the intralogistics environment with system transport demand and the dimensions of the mobile robots to automatically generate a roadmap for a homogeneous fleet of these robots. The environment is represented by geometric objects in continuous two-dimensional space, enabling high-fidelity modeling of real-world environments without the constraints of fixed spatial resolution. Map data may originate from CAD models, digital twins, or laser scanner data. In the latter case, post-processing is required to extract geometric

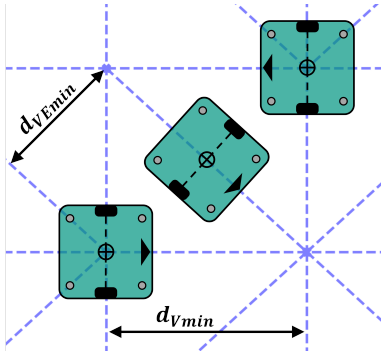


Fig. 2. Minimum distance constraints for roadmap nodes and edges based on mobile robot dimensions.  $d_{Vmin}$  denotes the minimum inter-node distance, and  $d_{VEmin}$  is the minimum node-edge distance.

features and convert environmental objects into polygonal representations [19], [20].

In the configuration space  $C$ , the state of a mobile robot is defined by its position  $x, y$  and orientation  $\theta$ . The subset of configurations where the robot collides with an obstacle is called the obstacle space  $C_{obs}$ . The set of all collision-free configurations, denoted as the free space  $C_{free}$ , is defined as:

$$C_{free} = C \setminus C_{obs}. \quad (1)$$

To compute the free space space, all geometric objects are expanded by the rotation radius of the robots  $r_{rob}$  plus an additional safety distance  $d_s$ , see Fig. 1. This expansion assumes that robots can rotate in place, as with a differential drive, where the rotation radius is measured from the robot center to its outermost point. The safety distance accounts for allowed path deviations, control imprecision and localization inaccuracies, ensuring collision-free operation.

The free space is used to generate navigable roadmaps. A graph  $G = (V, E)$  is defined, where all nodes and edges  $V, E \subset C_{free} \subseteq C$  are within the free space, as shown in Fig. 1. To ensure efficient utilization of the roadmap and simplify the coordination of mobile robots, additional geometric constraints are imposed on the roadmap. Initially, the graph must be planar. Furthermore, minimum inter-node and node-edge distance constraints are defined. The following minimum inter-node distance  $d_{Vmin}$  between any two nodes  $v_i, v_j \in V$ ,  $i \neq j$  in the graph  $G$  is introduced:

$$\|v_i - v_j\| \geq d_{Vmin} = 2 \cdot (r_{rob} + d_s). \quad (2)$$

This constraint ensures the simultaneous use of neighboring nodes by two mobile robots without mutual interference.

In addition, the minimum node-edge distance  $d_{VEmin}$  between an edge  $e = (v_i, v_j)$ , with  $v_i, v_j \in V$ ,  $i \neq j$ , and any node  $v_k \in V \setminus \{v_i, v_j\}$ , that is not an endpoint of the edge, is defined:

$$d(v_k, e) \geq d_{VEmin} = r_{rob} + \frac{w_{rob}}{2} + 2 \cdot d_s. \quad (3)$$

Here,  $d(v_k, e)$  is the Euclidean distance between an edge and a node that is not an endpoint of the edge.  $w_{rob}$  denotes the width of the mobile robots. This constraint assumes that edges represent straight-line connections between nodes, which the robots follow with a maximum deviation of  $d_s$ . It ensures that mobile robots occupying a node do not interfere with mobile robots moving along a not connected edge.

The defined geometrical constraints ensure efficient usage of the roadmap and are illustrated in Fig. 2. The mobile robots considered in this work are square-shaped, with a rotation radius of  $r_{rob} = 0.5$  m and a width of  $w_{rob} = 0.35$  m. A safety distance of  $d_s = 0.2$  m is assumed to ensure collision-free coordination of the mobile robots.

### III. AUTOMATED ROADMAP GENERATION

The proposed roadmap generation approach consists of a structured four-step process: (i) free space discretization, (ii) edge construction, (iii) roadmap optimization, and (iv) roadmap smoothing. Prior to these steps, a pre-processing stage defines the free configuration space  $C_{free}$  of the intralogistics environment. The environment is modeled using polygonal objects that represent the outer boundary, obstacles, and stations. While the outer boundary and obstacles are purely geometric, stations include one or more interaction points that serve as start and end points for transport tasks and may also act as geometric obstacles (see Fig.1 and Fig.5).

Besides the environment and the dimensions of the mobile robots, the transport demand of the system is considered in the proposed approach. It is represented by a transportation matrix  $T \in \mathbb{N}^{n \times n}$ , as shown in Table I for Environment 1, where  $n$  is the number of interaction points in the intralogistics environment. Each element  $T_{ij}$  specifies the number of transport tasks per time unit from interaction point  $i$  to  $j$ . The transportation matrix includes both loaded and empty runs.

TABLE I  
TRANSPORTATION MATRIX OF ENVIRONMENT 1 INDICATING TRANSPORT DEMAND BETWEEN STATION INTERACTION POINTS PER TIME UNIT.

From\To	1	2	3	4	5	6
1	0	3	0	3	3	3
2	3	0	3	0	0	0
3	0	3	0	3	3	3
4	3	0	3	0	0	0
5	3	0	3	0	0	0
6	3	0	3	0	0	0

#### A. Free Space Discretization

The objectives of the discretization of the free space are: (i) to enable short path connections between station interaction points, (ii) to flexibly adapt to the geometric characteristics of arbitrarily shaped polygonal environments, and (iii) to ensure efficient utilization of the available free space.

Since transport tasks are performed between interaction points, nodes are first placed at these specific positions  $(x, y)$  in the environment. Let  $V_{st}$  denote the set of nodes representing these interaction points. Next, convex corner points of the free space are extracted, as they represent key geometric

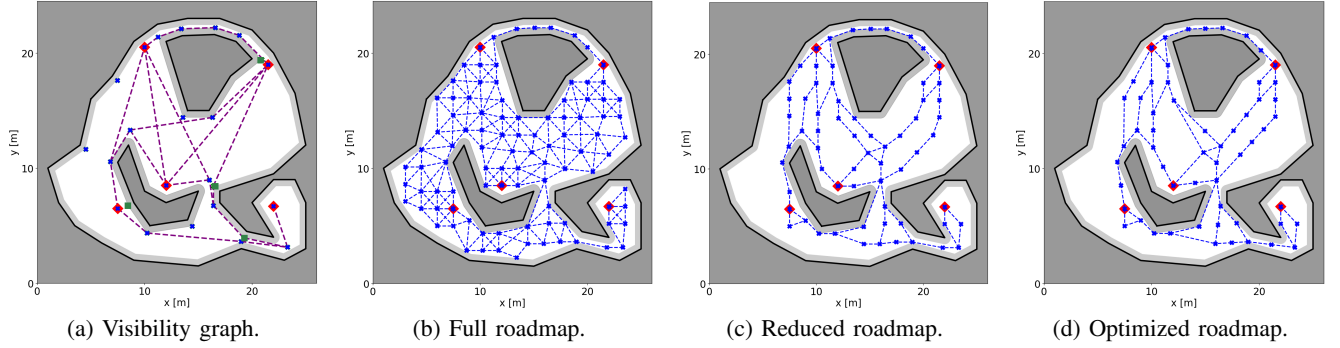


Fig. 3. Automated roadmap generation process shown for an abstract environment. (a) Visibility graph connecting the interaction points of the environment for a uniform transport demand, with added (blue crosses) and not added nodes (green squares). (b) Full roadmap after defining local grids and edge connections. (c) Reduced roadmap after pruning nodes and edges to adjust the redundancy. (d) Optimized roadmap after removing crossing edges and straightening paths.

features that support efficient space utilization and enable short connections between interaction points. These corner points are part of the visibility graph, which defines the Euclidean shortest paths within  $C_{\text{free}}$  between the interaction points [21].

Nodes are placed at convex corner points, provided the minimum inter-node distance  $d_{V_{\text{min}}}$  is not violated. When this constraint prevents placement, priority is given to corner points that contribute most centrally to the visibility graph connecting interaction points with non-zero transport demand.

An example of the result is illustrated in Fig. 3a for an abstract environment. The visibility graph corresponding to a uniform transport demand between the red highlighted interaction points is shown by purple dashed lines. Blue crosses indicate the added nodes  $v \in V_{\text{st}} \cup V_{\text{co}}$ , while green squares denote convex corner points excluded due to the minimum inter-node distance constraint.

To further increase node coverage within  $C_{\text{free}}$ , a systematic discretization of the free space is performed using local grids centered around existing nodes. Each local grid consists of a finite set of grid points arranged in a regular pattern around a central node  $v$  located at position  $(x, y)$ . For a grid resolution  $d_g$ , the neighboring grid points  $v'$  in an 8-connected local grid are defined as:

$$v' \in \{(x + i \cdot d_g, y + j \cdot d_g) \mid i, j \in \{-1, 0, 1\}, (i, j) \neq (0, 0)\} \quad (4)$$

where  $i$  and  $j$  denote the relative grid shifts in  $x$ - and  $y$ -direction. The size of a local grid refers to the maximum absolute values of  $i$  and  $j$ .

Local grids are initialized at all nodes  $v \in V_{\text{st}} \cup V_{\text{co}}$ , with priority given to interaction points. Starting from a local grid of size 1, the grid size is iteratively increased until the free space is densely covered. The maximum grid size is determined based on the dimensions of the environment.

Two key distance constraints are enforced throughout this process: (i) Only those grid points that lie within  $C_{\text{free}}$  and respect the minimum inter-node distance  $d_{V_{\text{min}}}$  of Eq. (2) are added to the graph. (ii) The grid resolution  $d_g$  is selected such

that diagonal node connections meet the minimum node-edge distance constraint  $d_{VE_{\text{min}}}$  defined in Eq. (3).

This process results in well-distributed node placement with high coverage of the free space, respecting geometric features of the environment and distance constraints. Consequently, the key nodes  $v \in V_{\text{st}} \cup V_{\text{co}}$  exhibit strong connectivity, which enhances the roadmaps redundancy between stations.

### B. Edge Construction

To generate a full roadmap, nodes are connected by edges, each representing a bidirectional, straight-line connection between two distinct nodes. An edge  $e = (v_i, v_j)$  with  $v_i, v_j \in V$ , where  $i \neq j$ , is added to the graph only if two conditions are met: (i) The edge lies entirely within the free space:  $e \subset C_{\text{free}}$ . (ii) The edge maintains a minimum clearance  $d_{VE_{\text{min}}}$  from all nodes  $v_k \in V \setminus \{v_i, v_j\}$  that are not its endpoints, as required by Eq. (3).

These constraints may result in a non-planar graph, where edges are crossing, as shown in Fig. 3b. This is done deliberately to increase connectivity and will be addressed in the subsequent roadmap optimization step.

Edge directionality is not enforced. While unidirectional edges can support congestion control by regulating traffic flow, they also restrict routing flexibility and may increase the shortest path lengths between stations. In contrast, bidirectional edges preserve maximal routing flexibility and minimize travel distances. Therefore, the assignment of edge directions is deferred to the fleet management system, which can dynamically define them based on traffic policies, traffic zones, or real-time system conditions.

### C. Roadmap Optimization

The full roadmap is optimized using the transportation matrix of the intralogistics environment to reduce its complexity and adapt it to the transport demand. The optimization pursues three objectives: (i) maintaining sufficient redundancy between interaction points based on transport demand, (ii) pruning irrelevant nodes and edges to increase query efficiency, and (iii) minimizing transport distances between interaction points.

To identify relevant nodes and edges, Yen’s  $K$ -shortest path algorithm [22] is employed. For each pair of interaction points with non-zero transport demand ( $T_{ij} > 0$ ), a set of  $k$  loop-less redundant paths is computed.

A path  $p = (v_1, v_2, \dots, v_n)$  in the roadmap graph  $G = (V, E)$  is an ordered sequence of distinct nodes  $v_1, v_2, \dots, v_n \in V$  such that each consecutive pair of nodes  $(v_i, v_{i+1}) \in E$ , for  $i = 1, \dots, n - 1$ , is an edge of the graph. The sets of nodes and edges along a path  $p$  are denoted  $V_p$  and  $E_p$ , respectively.

The number of redundant paths  $k$  is chosen based on the quantity of transport tasks  $T_{ij}$  between a pair of interaction points. The time unit is adjusted to achieve a suitable level of redundancy. In contrast to the classic Yen’s algorithm, edge costs are dynamically updated during computation. After each path is found, the cost of every edge  $e \in E_p$  is multiplied by a penalty coefficient  $\gamma = 1.1^{u_{ij}(e)}$ , where  $u_{ij}(e) \in \mathbb{N}$  is a local usage counter that records how often edge  $e$  has been used in previously computed paths for the pair  $(i, j)$ . This biases subsequent searches toward alternative, less overlapping paths. After all  $k$  paths for a given pair are computed, edge costs are reset to  $\gamma = 1$ .

Let  $V_{ksp} \subseteq V$  and  $E_{ksp} \subseteq E$  denote the sets of all nodes and edges used across all  $k$ -shortest path computations. Additionally, a global usage counter  $u(e) \in \mathbb{N}$  is maintained for each edge  $e \in E_{ksp}$  to record the total number of times it appears in the computed paths.

The roadmap is pruned by removing all unused nodes  $v \in V \setminus V_{ksp}$  and edges  $e \in E \setminus E_{ksp}$ . This significantly reduces the graph complexity while preserving required redundancy. The reduced roadmap is illustrated in Fig. 3c.

To ensure planarity, all crossing edges in  $E_{ksp}$  are identified. For each edge  $e \in E_{ksp}$  that crosses others, an importance factor  $I(e)$  is computed:

$$I(e) = u(e) - \sum_{e' \in C(e)} u(e'), \quad (5)$$

where  $C(e) \subset E_{ksp}$  denotes the set of edges that geometrically cross  $e$ . The edge with the highest  $I(e)$  in each conflict group is retained, while all others are removed. This ensures preservation of the relevant edges that contribute most frequently to transport tasks.

An additional refinement is applied to further optimize the roadmap: (i) Nodes with only a single connected edge, except for  $v \in V_{st}$ , are removed along with their connected edges. (ii) Chains of nodes connected by two edges are replaced by a single, straight edge connection, provided the minimum node-edge distance constraint is satisfied. Subsequently, intermediate nodes are reinserted if the minimum inter-node distance constraint is met.

This final optimization step aim to generate roadmap with direct connections and short edge lengths, which minimizes path lengths the spatial footprint of reserved nodes and edges, supporting efficient fleet coordination. The resulting optimized roadmap is shown in Fig. 3d.

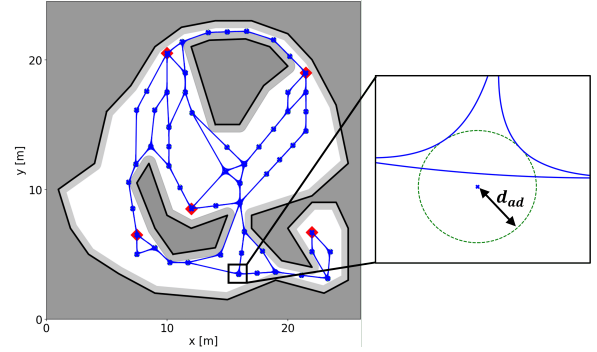


Fig. 4. Optimized roadmap with smooth trajectories. Blue lines show the smoothed roadmap generated using cubic splines, respecting the allowed deviation margin  $d_{ad}$  from nodes, represented by the green dotted circle.

#### D. Roadmap Smoothing

As a final step, the roadmap is smoothed to enable more efficient trajectories for mobile robots. This smoothing process is supported by the previous steps through the consideration of a safety distance  $d_s$ , which accounts for allowed deviations from planned paths  $d_{ad}$ , as well as localization inaccuracies and control imprecision.

By allowing controlled deviations from node positions and edge connections, smooth trajectories, such as those generated using cubic splines, can be planned directly on top of the roadmap. These smoothed paths locally approximate the discrete roadmap while respecting the allowed deviation margin  $d_{ad}$ . As illustrated in Fig. 4, this enables continuous and feasible routing through the environment without abrupt changes in direction at the nodes. The result is a roadmap that not only ensures redundancy and query efficiency but also supports smooth trajectory generation with bounded deviations.

## IV. EVALUATION METHODOLOGY

To evaluate the proposed roadmap generation approach, three intralogistics environments of varying scale and complexity are utilized, which are shown in Fig. 5. These environments have been adopted from literature, ensuring both reproducibility and relevance. Their spatial dimensions have been rescaled to match the size of the mobile robots used in this work. For each environment, a transportation matrix is defined to allow evaluation of specific intralogistics use cases.

- **Environment 1**, adapted from [12], represents a small-scale industrial setting with bidirectional transport tasks between two central storage points (1, 3) and four workstations (2, 4, 5, 6), as can be seen in Table I.
- **Environment 2**, based on [10], models a medium-scale matrix production system with multiple production cell types, allowing the evaluation of structured yet flexible transport flows, typical of modular and reconfigurable production environments. The transportation matrix induces a material flow from left to right through the system with empty runs in the opposite direction.
- **Environment 3**, adapted from [13], which is also used in [1], represents a large-scale industrial setting char-

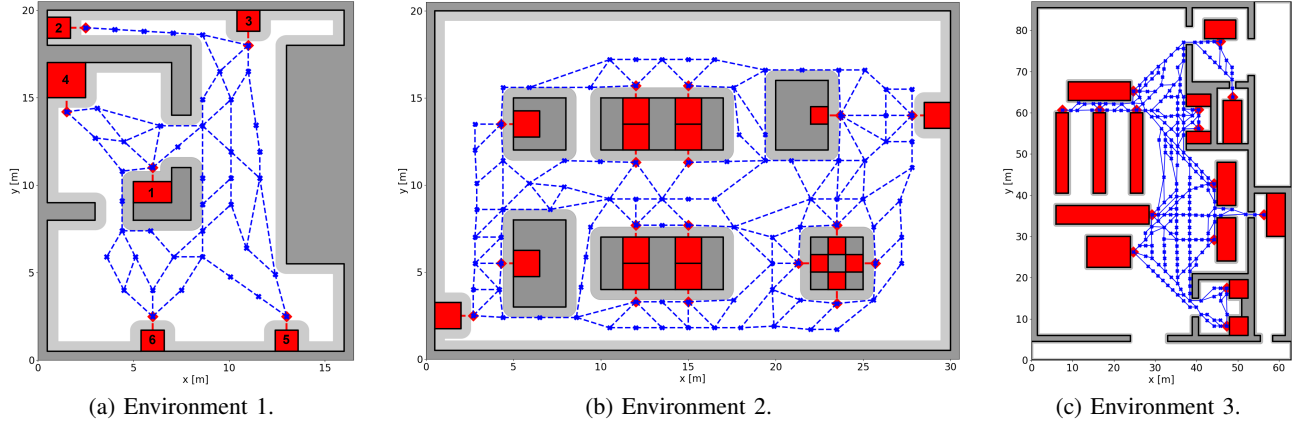


Fig. 5. Intralogistics environments used for evaluation. Red areas are stations with their interaction points marked by red rhombuses. The optimized roadmaps using the proposed approach are visualized by the blue crosses and blue dashed lines.

acterized by numerous stations, with uniform transport tasks between them. It supports the evaluation of complex systems with high-volume transportation tasks.

To benchmark the performance of the generated roadmaps, comparative roadmaps are generated for each of the three environments using established baseline approaches. The following discretization strategies are employed:

- **4-connected grid:** Nodes are placed on a regular grid based on the minimum node distance defined in Eq. (2), with edges connecting horizontal and vertical neighbors.
- **8-connected grid:** Similar to the 4-connected grid, but with increased node spacing to allow diagonal edge connections, satisfying the distance constraint from Eq. (3).
- **Random sampling:** Nodes are placed at random within the free space, ensuring a minimum node distance according to Eq. (2).

After discretizing the free space, edge connections are defined using the Delaunay triangulation [23], in contrast to the edge construction method presented in this paper. This produces a well-connected planar graph while avoiding narrow angles between edges. To ensure comparable redundancy between the proposed and the three baseline approaches, edges are reduced using Yen's algorithm, see Section III-C, corresponding to step (b) to (c) in Fig. 3 but not to (d), which would alter the initial node positions. For Environment 1, the resulting roadmaps are compared in Fig. 6.

Graph-theoretical metrics are used to evaluate the performance of the roadmaps, following the methodology in [5], [16], [17] and [3]. These chosen metrics assess structural complexity, roadmap redundancy, and routing efficiency:

- **Number of nodes and edges:** Evaluates the structural complexity of the roadmap, which affects the query efficiency of routing algorithms.
- **Number of expanded nodes:** Measures the query efficiency of the roadmap using the A\* algorithm with an Euclidean heuristic. Paths between all interaction points with non-zero transport demand are computed, and the total number of expanded nodes is recorded.

- **Mean node and edge connectivity:** Evaluates the mean minimum number of nodes or edges that must be removed to disconnect two interaction points with non-zero transport demand. These metrics provide an indication of the robustness and redundancy of the roadmap [17].
- **Algebraic connectivity:** The second-smallest eigenvalue of the Laplacian of the graph, reflects the overall connectivity of the roadmap [5].
- **Alpha, beta, and gamma index:** Global graph-theoretical measures of redundancy and connectivity [24], defined as  $\alpha = \frac{|E|-|V|+1}{2|V|-5}$ ,  $\beta = \frac{|E|}{|V|}$ ,  $\gamma = \frac{|E|}{3(|V|-2)}$ .
- **Normalized mean shortest path length:** Evaluates routing efficiency by measuring the mean length of the shortest path between each pair of interaction points with non-zero transport demand. This value is normalized using the mean Euclidean shortest path length.

## V. EVALUATION AND RESULTS

Table II summarizes the quantitative evaluation of the proposed roadmap generation approach (own) against three baseline approaches across intralogistics environments of varying complexity, using graph-theoretical metrics. For the stochastic random sampling baseline, results are reported as the mean over ten runs, given the minimal observed variability. A qualitative visual comparison for Environment 1 is shown in Fig. 6. The subsequent analysis focuses on three aspects: structural complexity, roadmap redundancy, and routing efficiency.

The proposed approach consistently generates roadmaps with the lowest structural complexity. Relative to the 8-connected grid, node and edge counts are reduced on average by 14.9 % and 9.6 %, respectively, with reductions increasing to 47.0 % and 40.0 % compared to the 4-connected grid. Against the random sampling baseline, reductions of 26.5 % for nodes and 18.1 % for edges are observed. This reduction in structural complexity leads into measurable performance improvements: Across all pairs of interaction points with non-zero transport demand of all three environments, the A\* algorithm expands on average 27.5 % fewer nodes, indicating that

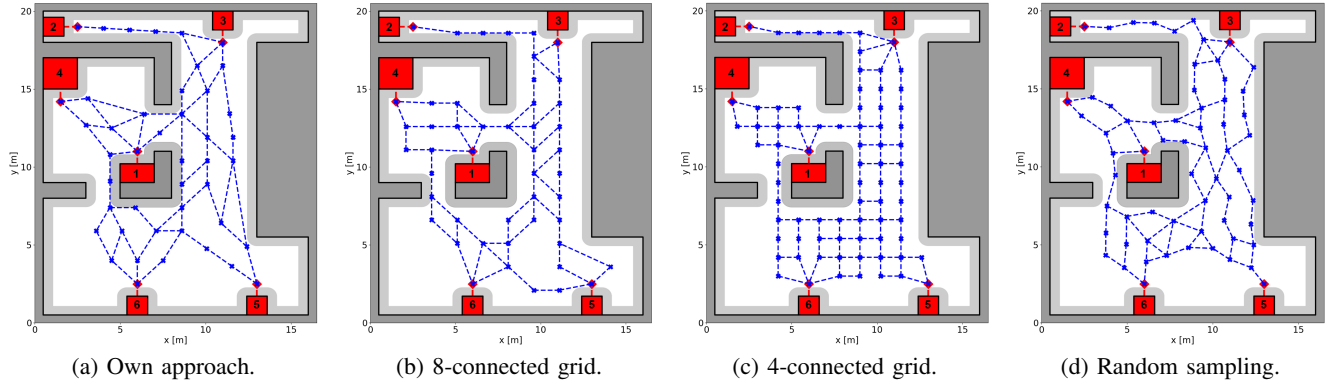


Fig. 6. Comparison of the generated roadmaps of the proposed approach and the three baseline approaches for Environment 1. The optimized roadmaps are visualized by the blue crosses and blue dashed lines.

TABLE II  
EVALUATION OF THE PROPOSED ROADMAP GENERATION APPROACH AGAINST THREE BASELINE APPROACHES ACROSS THREE ENVIRONMENTS USING GRAPH-THEORETICAL METRICS. GREEN CELLS INDICATE THE BEST VALUE FOR EACH METRIC IN EACH ENVIRONMENT.

metrics	Env. 1				Env. 2				Env. 3				ideal
	own	8-grid	4-grid	rand.	own	8-grid	4-grid	rand.	own	8-grid	4-grid	rand.	
number of nodes	44	48	77	63	94	104	185	150	250	341	491	284	min
number of edges	64	67	107	84	157	163	255	214	351	457	600	365	min
expanded nodes A* alg.	265	291	467	359	568	742	1098	857	9572	11079	14863	11153	min
mean node connectivity	1.750	1.750	1.825	1.5	2.714	2.143	2.357	2.036	1.744	1.553	1.591	1.265	max
mean edge connectivity	2.000	1.750	1.825	1.5	2.821	2.142	2.357	2.071	1.837	1.647	1.591	1.237	max
algebraic connectivity	0.127	0.076	0.038	0.052	0.099	0.049	0.016	0.025	0.013	0.006	0.002	0.007	1
alpha index	0.253	0.220	0.208	0.182	0.350	0.296	0.195	0.220	0.206	0.173	0.113	0.146	1
beta index	1.454	1.396	1.390	1.333	1.670	1.567	1.378	1.427	1.404	1.340	1.222	1.285	max
gamma index	0.508	0.486	0.475	0.459	0.569	0.533	0.464	0.482	0.471	0.449	0.409	0.431	1
norm. shortest path len.	1.046	1.137	1.176	1.150	1.033	1.148	1.174	1.235	1.044	1.064	1.202	1.121	1

lower graph complexity directly improves query efficiency, which is critical for real-time intralogistics applications.

Despite reduced complexity, the proposed approach enhances roadmap redundancy. Mean node and edge connectivity between interaction points with transport demand increase by 6.9 – 29.3 % and 14.9 – 39.4 %, respectively, relative to the baseline approaches, highlighting greater routing flexibility and robustness under high demand. Global connectivity metrics, including algebraic connectivity and the alpha, beta, and gamma indices, are also improved, achieving the highest scored across all three environments. This indicates that improvements extend beyond demand-specific paths and reflect a structurally more resilient roadmap. These results suggest that the proposed approach achieves a favorable trade-off between reduced complexity and increased redundancy and robustness.

Routing efficiency, measured using the normalized mean shortest path length, is consistently near the theoretical optimum of 1, ranging from 1.033 to 1.046 across all environments. Baseline approaches, in contrast, exhibit substantially longer paths with values ranging from 1.064 up to 1.235. This improvement is primarily achieved by incorporating convex corner points, capturing key geometric features of the environment, into the roadmap. These results indicate that the proposed approach not only enables flexible and redundant routing but also minimizes travel distances, with direct benefits for travel time and energy consumption in operational settings.

The evaluation demonstrates that the proposed roadmap generation approach effectively balances structural complexity and redundancy, producing roadmaps tailored to intralogistics applications. By reducing the number of nodes and edges while maintaining higher redundancy between interaction points, the approach achieves near-optimal path lengths and enhanced routing flexibility. The consistent improvements observed across all three environments indicate that the approach scales well and generalizes to diverse layout configurations, offering robust performance beyond what is guaranteed by baseline methods. These results suggest that the proposed method provides a practical solution for designing efficient and resilient virtual roadmaps in intralogistics systems.

Despite these promising results, several limitations should be noted. First, routing efficiency is heavily influenced by the fleet management system, which was not evaluated. The graph-theoretical metrics employed here serve as predictive indicators rather than direct measures of system-level performance. Second, redundancy was derived solely on the basis of the transport matrix and does not account for combinatorial interactions between conflicting transport routes. Finally, no direct comparison with existing literature was conducted, as specific intralogistics use cases were defined in this work, to which the roadmaps are tailored. Therefore, a direct comparison with the roadmaps presented in the literature is not meaningful, even if the same environments are used.

## VI. CONCLUSION

This paper introduces a continuous-space roadmap generation approach for mobile robot fleets. It successfully bridges the gap between geometrically constrained grid-based approaches and continuous-space approaches, which lack practical distance constraints. By integrating station-to-station transport demand and minimum distance constraints for nodes and edges directly into a continuous-space optimization process, the proposed approach combines the high-fidelity modeling of continuous-space approaches with large fleet capabilities of grid-based approaches.

Evaluation across three intralogistics environments demonstrates that the proposed approach outperforms established baselines, producing roadmaps with reduced structural complexity, higher redundancy between interaction points, and near-optimal path lengths. These results indicate that the approach supports fast, data-driven generation of tailored roadmaps, enhancing the flexibility, and adaptability of automated intralogistics systems.

Future work will quantify system-level performance, including throughput and task completion times, through lifelong multi-agent pathfinding simulations and benchmark the approach against state-of-the-art methods on identical intralogistics use cases to enable meaningful comparisons. In addition, a zone concept will be integrated to mitigate potential conflicts between mobile robots, and charging infrastructure will be incorporated, further extending the practical applicability of the approach.

## REFERENCES

- [1] T. Žužek, R. Vrabčič, A. Zdešar, G. Škulj, I. Banfi, M. Bošnjak, V. Zaletelj, and G. Klančar, "Simulation-based approach for automatic roadmap design in multi-AGV systems," *IEEE Transactions on Automation Science and Engineering*, vol. 21, no. 4, pp. 6190–6201, Oct. 2023.
- [2] L. Sabattini, V. Digani, C. Secchi, G. Cotena, D. Ronzoni, M. Foppoli, and F. Oleari, "Technological roadmap to boost the introduction of AGVs in industrial applications," in *2013 IEEE 9th International Conference on Intelligent Computer Communication and Processing (ICCP)*. Cluj-Napoca, Romania: IEEE, Oct. 2013, pp. 203–208.
- [3] C. Henkel, M. Toussaint, and W. Hönig, "GSRM: Building Roadmaps for Query-Efficient and Near-Optimal Path Planning Using a Reaction Diffusion System," in *2024 IEEE/RSJ International Conference on Intelligent Robots and Systems*. Abu Dhabi, United Arab Emirates: IEEE, 2024, pp. 10 694–10 701.
- [4] I. Petrovic, E. Menegatti, I. Marković, R. Vrabčič, T. Žužek, G. Škulj, I. Banfi, and V. Zaletelj, "Improving the flow in multi-robot logistic systems through optimization of layout roadmaps," in *Intelligent Autonomous Systems 17*. Cham: Springer, 2023, vol. 577, pp. 923–934.
- [5] V. Digani, L. Sabattini, C. Secchi, and C. Fantuzzi, "An automatic approach for the generation of the roadmap for multi-AGV systems in an industrial environment," in *2014 IEEE/RSJ International Conference on Intelligent Robots and Systems*. Chicago, IL, USA: IEEE, 2014, pp. 1736–1741.
- [6] R. Geraerts and M. H. Overmars, "A comparative study of probabilistic roadmap planners," in *Algorithmic Foundations of Robotics V*, J.-D. Boissonnat, J. Burdick, K. Goldberg, and S. Hutchinson, Eds. Berlin, Heidelberg: Springer, 2004, vol. 7, pp. 43–57.
- [7] T. Asano, T. Asano, L. Guibas, J. Hershberger, and H. Imai, "Visibility-polygon search and euclidean shortest paths," in *26th Annual Symposium on Foundations of Computer Science (sfcs 1985)*. Portland, OR, USA: IEEE, 1985, pp. 155–164.
- [8] S. M. LaValle, "Rapidly-exploring random trees: A new tool for path planning," *The annual research report*, 1998.
- [9] J. O. Wallgrün, "Autonomous construction of hierarchical Voronoi-based route graph representations," in *Spatial Cognition IV. Reasoning, Action, Interaction*, D. Hutchison, T. Kanade, J. Kittler, J. M. Kleinberg, and F. Mattern, Eds. Berlin, Heidelberg: Springer, 2005, vol. 3343, pp. 413–433.
- [10] D. Kozjek, A. Malus, and R. Vrabčič, "Reinforcement-learning-based route generation for heavy-traffic autonomous mobile robot systems," *Sensors*, vol. 21, no. 14, p. 4809, 2021. [Online]. Available: <https://www.mdpi.com/1424-8220/21/14/4809>
- [11] R. Vrabčič, A. Malus, J. Dvoršak, G. Klančar, and T. Žužek, "Bio-Inspired Traffic Pattern Generation for Multi-AMR Systems," *Applied Sciences*, vol. 15, no. 5, p. 2849, 2025.
- [12] S. Uttendorf and L. Overmeyer, "Fuzzy-enhanced path-finding algorithm for AGV roadmaps," in *Conference of International Fuzzy Systems Association and European Society for Fuzzy Logic and Technology*, Gijón, Spain, 2015.
- [13] S. Uttendorf, B. Eilert, and L. Overmeyer, "A fuzzy logic expert system for the automated generation of roadmaps for automated guided vehicle systems," in *2016 IEEE International Conference on Industrial Engineering and Engineering Management (IEEM)*. Bali, Indonesia: IEEE, 2016, pp. 977–981.
- [14] I. Bang, B.-I. Kim, and Y. Kim, "Virtual grid layout with direction constraints for autonomous mobile robot routing performance improvement," *International Journal of Advanced Manufacturing Technology*, vol. 128, no. 9-10, pp. 4653–4665, 2023.
- [15] A. Kleiner, D. Sun, and D. Meyer-Delius, "ARMO: Adaptive road map optimization for large robot teams," in *2011 IEEE/RSJ International Conference on Intelligent Robots and Systems*. San Francisco, CA, USA: IEEE, 2011, pp. 3276–3282.
- [16] J. Stenzel, D. Lunsch, and L. Schmitz, "Automated topology creation for global path planning of large AGV fleets," in *2021 IEEE International Intelligent Transportation Systems Conference (ITSC)*. Indianapolis, IN, USA: IEEE, 2021, pp. 3373–3380.
- [17] J. Stenzel and L. Schmitz, "Automated roadmap graph creation and MAPF benchmarking for large AGV fleets," in *2022 8th International Conference on Automation, Robotics and Applications (ICARA)*. Prague, Czech Republic: IEEE, 2022, pp. 146–153.
- [18] C. Henkel and M. Toussaint, "Optimized directed roadmap graph for multi-agent path finding using stochastic gradient descent," in *Proceedings of the 35th Annual ACM Symposium on Applied Computing*. Brno, Czech Republic: ACM, Mar. 2020, pp. 776–783.
- [19] H. A. Aryadi, R. Bezerra, K. Ohno, K. Gunji, S. Kojima, M. Kuwahara, Y. Okada, M. Konyo, and S. Tadokoro, "Redundant Voronoi Roadmap Graph Using Imaginary Obstacles for Multi-Robot Path Planning," in *2023 IEEE International Conference on Systems, Man, and Cybernetics (SMC)*. Honolulu, Oahu, HI, USA: IEEE, 2023, pp. 1772–1779.
- [20] P. Beinschob, M. Meyer, C. Reinke, V. Digani, C. Secchi, and L. Sabattini, "Semi-automated map creation for fast deployment of AGV fleets in modern logistics," *Robotics and Autonomous Systems*, vol. 87, pp. 281–295, Jan. 2017.
- [21] S. M. LaValle, *Planning Algorithms*, 1st ed. Cambridge University Press, 2006. [Online]. Available: <https://www.cambridge.org/core/product/identifier/9780511546877/type/book>
- [22] J. Y. Yen, "Finding the  $K$  Shortest Loopless Paths in a Network," *Management Science*, vol. 17, no. 11, pp. 712–716, Jul. 1971.
- [23] B. N. Delaunay, "Sur la sphère vide," *Bulletin of Academy of Sciences of the USSR*, vol. 7, no. 6, pp. 793–800, 1934.
- [24] K. J. Kansky, "Structure of transportation networks : relationships between network geometry and regional characteristics," Dissertation, University of Chicago, 1963.